

Modeling Study of High Fuel Utilization In Solid Oxide Fuel Cell

Vishal Bhanudas Pawar

A Thesis Submitted to
Indian Institute of Technology Hyderabad
In Partial Fulfillment of the Requirements for
The Degree of Master of Technology



भारतीय प्रौद्योगिकी संस्थान हैदराबाद
Indian Institute of Technology
Hyderabad

Department of Chemical Engineering

June 2015

Declaration

I declare that this written submission represents my ideas in my own words, and where others' ideas or words have been included, I have adequately cited and referenced the original sources. I also declare that I have adhered to all principles of academic honesty and integrity and have not misrepresented or fabricated or falsified any idea/data/fact/source in my submission. I understand that any violation of the above will be a cause for disciplinary action by the Institute and can also evoke penal action from the sources that have thus not been properly cited, or from whom proper permission has not been taken when needed.

Pawar

(Signature)

Vishal Bhanudas Pawar.

(Vishal Bhanudas Pawar)

CH13M1016

(Roll No)

Approval Sheet

This thesis entitled Modeling Study of High Fuel Utilization of in Solid Oxide Fuel Cell by Vishal Bhanudas Pawar is approved for the degree of Master of Technology from IIT Hyderabad.



Dr. Parag Pawar
Assistant Professor
Dept. of Chemical Engineering
Indian Institute of Technology Hyderabad
Internal Examiner



Dr. Vinod Janardhanan
Associate Professor
Dept. of Chemical Engineering
Indian Institute of Technology Hyderabad
Internal Examiner



Dr. Dayadeep Monder
Assistant Professor
Dept. of Energy Science and Engineering
Indian Institute of Technology Bombay
Adviser



Dr. Raja Banerjee
Associate Professor
Dept. of Mechanical and Aerospace Engineering
Indian Institute of Technology Hyderabad
External Examiner

Acknowledgements

I wish to express my special appreciation and thanks to my advisor Dr. Dayadeep Monder, have been tremendous mentor for me. I would like to thank you for encouraging my research. Your advice on both research as well as on my career have been price less.

I would like to thank my committee members, Dr. Vinod Janaradhanan, Dr. Phanindra Verma Jampana, Dr. Parag D Pawar.

I am also grateful to the Department of Chemical Engineering, Indian Institute of Technology Hyderabad. I would like to thank Mr. Rustam Singh Shekhar at IIT Bombay and Mr. V. Goutham Pollisetty at IIT Hyderabad. All of you have been there to support me.

Dedication

TO MY PARENTS

Abstract

Solid Oxide Fuel Cell offers higher conversion efficiency compared to all other fuel cells. Fuel cell technology is also a cleaner alternative where particulate and NO_x emissions can be essentially eliminated and the carbon emissions per unit of electrical energy are much lower. This work aims to use simulations from a detailed coupled multiphysics model to identify and evaluate desirable operating regions for a SOFC. We are interested in maximizing fuel utilization, cell efficiency as well as power density without going into operating regions where degradation modes such as Ni oxidation become active. In this study, we present a series of parametric studies by simulating the model at different flow-rates, fuel compositions, temperatures and cell voltages. The SOFC geometry used here is an anode supported planar cell with counter-current flow of air and fuel ($H_2 - H_2O$ mixtures). The model used is a 2D fully coupled transport-reaction model implemented in COMSOL Multiphysics.

Our model includes fluid flow and species balance equations in the porous electrodes and flow channels coupled with the electronic and ionic potential distribution equations in the electrodes and electrolyte.

Our results show that there is risk of Ni oxidation only at very high fuel utilization (U_f). However, the threshold U_f is a function of a) cell voltage, b) inlet fuel composition, and c) operating temperature.

Contents

Declaration	ii
Approval Sheet	iv
Acknowledgements	v
Abstract	vii
Nomenclature	ix
1 Introduction	4
1.1 Fuel Cells	4
1.2 Solid oxide fuel cells	5
1.2.1 Anode	6
1.2.2 Cathode	6
1.2.3 Electrolyte	6
1.3 Scope of the thesis	7
2 Physics and Model Equation	8
2.1 Physics and thermodynami	8
2.1.1 SOFC Thermodynemics	8
2.1.2 Voltage losses in SOFC	9
2.1.3 Redox reaction in anode	10
2.2 Flow equations and Boundary conditions	11
2.2.1 Flow in gas channels and electrode	11
2.3 Mass Trasnfer in the channels and electrodes	11
2.4 Voltage and Current Distribution	12
2.4.1 Effective Conductivity	13
2.4.2 Peclet number and Back diffusion	14

2.4.3	Electrochemistry	15
2.5	Ni oxidation thermodynamics	16
3	Model Implementation	19
3.1	Geometry and Mesh	19
3.3	Solver Used	20
3.2	Parameter	21
4	Results and Discussion	22
4.1	$H_2 : H_2O = 0.97:0.03$	22
5	Conclusion	34

List of Figures

1.1	Solid Oxide Fuel Cell	5
2.1	Flux ratio versace Peclet number	14
2.2	Scale for the ΔG and (Q/K) showing the spontaneous change of a chemical reaction	18
3.1	2D planar cell	19
3.2	fuel cell 2-D section of actual simulated geometry	19
3.3	2D planar cell meshing	20
4.1	Mole Fraction of H_2 , current generation and partial pressure along the length of cell at 700°C	23
4.2	Mole Fraction of H_2 , current generation and partial pressure along the length of cell at 750°C	23
4.3	Mole Fraction of H_2 , current generation and partial pressure along the length of cell at 800°C	24
4.4	Safe and Unsafe region for 700°C	24
4.5	Safe and Unsafe region for 750°C	25
4.6	Safe and Unsafe region for 800°C	25
4.7	Mole Fraction of H_2 , current generation and partial pressure along the length of cell at 700°C	26
4.8	Mole Fraction of H_2 , current generation and partial pressure along the length of cell at 750°C	27
4.9	Mole Fraction of H_2 , current generation and partial pressure along the length of cell at 800°C	28
4.10	Safe and Unsafe region for 700°C	29
4.11	safe and Unsafe region for 750°C	29

4.12 Safe and Unsafe region for 800 ⁰ C	30
4.13 Safe and Unsafe region for 700 ⁰ C at H_2 25%	30
4.14 Safe and Unsafe region for 800 ⁰ C at H_2 25%	31
4.15 Fuel cell efficiency as function of cell voltage at a given utilization at 700 ⁰ C	32
4.16 Fuel cell efficiency as function of cell voltage at a given utilization at 750 ⁰ C	32
4.17 Fuel cell efficiency as function of cell voltage at a given utilization at 800 ⁰ C	33

List of Tables

3.1	These are the parameters	21
-----	------------------------------------	----

Chapter 1

Introduction

1.1 Fuel Cells

A Fuel Cell is an electrochemical device which can convert chemical energy directly into electrical energy. With increasing demand for electricity, dependence on fossil fuels like coal, natural gas and oil to meet the demand also increases. Current electricity generation methods have significant health and environmental impacts, so we need to look at alternatives for these. Fuel cell Technology is clean technology which generates electricity from hydrogen with water as a product. Fuel cell are different from batteries, a battery stores chemical reactants whereas a fuel cell is continuously supplied with fuel to generate electricity. Fuel cell can produce electricity as long as it has fuel supply. Fuel cell have been used in many other application like primary and backup power for industrial, commercial and residential buildings and remote and inaccessible areas.

There are many types of fuel cells which are as follows:

1. Polymer electrolyte membrane fuel cells
2. Alkaline fuel cells
3. Phosphoric acid fuel cells
4. Molten carbonate fuel cells
5. Solid oxide fuel cells

These fuel cells are differentiated based on the operating temperature and electrolyte. [1]

1.2 Solid oxide fuel cells

Solid Oxide Fuel Cell (SOFC) is an electrochemical which converts chemical energy into electrical energy. It has high efficiency compared to all other fuel cell. Advantages SOFC are high efficiency, long-term stability, fuel flexibility, low emission and relatively low cost. One disadvantage is its high operating temperatures which in longer start-up times and mechanical chemical stability issues. Fuel flexibility of SOFC allows it to be operated with variety of fuels including hydrogen, carbon monoxide, hydrocarbon and mixture of these.

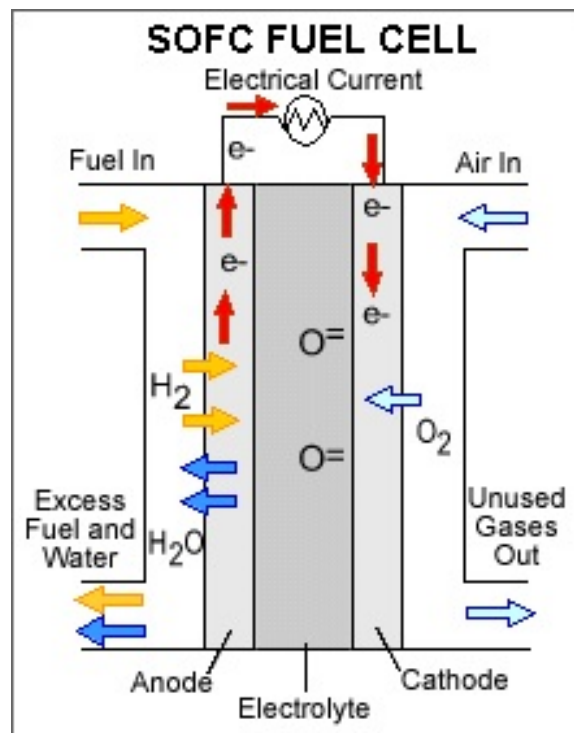
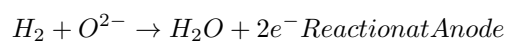
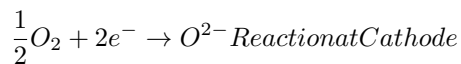


Figure 1.1: Solid Oxide Fuel Cell

If we start from fuel channel, the fuel has to be transported to reaction sites which lie at the interface of the fuel, anode catalyst, and electrolyte material and that interfacial active sites are called triple phase boundary (TPB). Oxidation takes place at anode and reduction takes place at cathode the reaction at anode and cathode are as follows.





1.2.1 Anode

In SOFC most common anode material used is cermet (Ni-YSZ). Ni is a good electronic conductor and YSZ is an ionic conducting material and it has high mechanical and chemical stability. Ni is catalyst for hydrogen oxidation reaction. The porous nature of cermet allows transport of gas species through it. The composite structure which is composed of micron scale Ni and YSZ particle has electrochemically active three phase boundary sites throughout. The nickel oxide in anode is generally reduced to nickel prior to the first operation. Once exposed to air under the cell operating temperature, the Ni-YSZ cermet anode can be oxidized. It is known that redox of the anode is detrimental to the cell performance. Cyclic redox is likely to occur during SOFC operation so the bulk volume of a fully dense NiO sample should contract by 40.9% upon reduction and should expand by 69.2% upon oxidation.

1.2.2 Cathode

The material used for cathode is a porous composite mixture of lanthanum strontium manganite (LSM) and yttria-stabilized zirconia (YSZ). LSM is denoted as $La_{1-x}Sr_xMnO_3$, where x describes the doping level and x varies from 10 to 20 percent. At higher operating temperature, LSM has high electric conductivity and low ionic conductivity.

1.2.3 Electrolyte

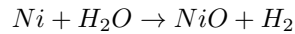
Electrolyte used in SOFCs is yttria-stabilized zirconia (YSZ). YSZ can be used safely even at operating temperatures greater than 750°C. Characteristics of YSZ are low ionic resistivity, very high electronic resistivity, and good chemical stability in highly oxidizing as well as reducing atmosphere. We use a very thin layer of electrolyte to reduce ohmic losses.

1.3 Scope of the thesis

Our focus in current work is to find out a safe operating zone for SOFC operation by simulating a multiphysics model of an SOFC in COMSOL. The 2D and 3D models incorporate various transport and electrochemical processes in an SOFC and the associated PDEs are solved.

We have developed a detail model and used it to perform a series of parametric studies that help us better understand the coupling of the various physics. In chapter 2 we will discuss the model physics and present the details of model developed which will include the partial differential equations, the boundary condition and the solution method used. In chapter 3 we will present the geometry of the SOFC, parameters in modeling and meshing details.

In SOFC, Hydrogen is used as a fuel which is costly so one has to used this fuel efficiently and precisely. If fuel cell works with high fuel flow rates it will give high current but there is wastage of fuel. At low velocities, though fuel utilization is high nickel oxidation will take place which is not desirable. Formation of Nickel Oxide results in deterioration of anode.



Nickel oxide is in solid thin film form, during the fuel cell operation this film spread on anode electrode during the operation which reduce the porosity of anode and over a period of time anode will deteriorate. Performance and efficiency of an SOFC depends on anode electrode.

Chapter 2

Physics and Model Equation

2.1 Physics and thermodynamics

2.1.1 SOFC Thermodynamics

This section outlines the relationship between Gibbs free energy and the maximum electrical potential for the cell: Nernst equation.

Gibbs free energy calculation

Gibbs free energy is the work potential of the reaction which relates to change in enthalpy and entropy for the reaction.

$$\Delta G = \Delta H - T\Delta S \quad (2.1)$$

Relation between Gibbs free energy and voltage

Work done by fuel cell is electrical work.

$$W = qE \quad (2.2)$$

$$q = nF \quad (2.3)$$

$$W = nFE \quad (2.4)$$

Here q is charge transfer, F is Faraday's constant, n is number of electrons transferred in the reaction and E is the electric potential

From the first law of thermodynamic $\Delta H = Q - W$ for a reversible process.

$$Q = T\Delta S \quad (2.5)$$

$$\Delta H = T\Delta S - nFE \quad (2.6)$$

$$\Delta H - T\Delta S = \Delta G = -nFE \quad (2.7)$$

$$E = \frac{-\Delta G_{rxn}}{nF} \quad (2.8)$$

This is equivalent to Nernst equation. E is reversible voltage for reaction. If reactant and product are in standard state then,

$$E^0 = \frac{-\Delta G_{rxn}}{nF} \quad (2.9)$$

The variation of reversible voltage with temperature T can be calculated as:

$$E^0(T) = E^0(T^0) + \frac{-\Delta S^0}{nF}(T - T^0) \quad (2.10)$$

If ΔS^0 is negative, $E^0(T)$ decrease with an increase with and temperature T.

Nernst Equation

$$E = E^0 - \frac{RT}{nF} \ln \frac{\prod a_{product}^{v_i}}{\prod a_{reactant}^{v_i}} \quad (2.11)$$

This equation relates the equilibrium potential to the standard potential, temperature and pressure/concentration of reactant and product.

2.1.2 Voltage losses in SOFC

Operating voltage of SOFC is less than the Nernst voltage due to voltage losses in the electrode and electrolyte caused by reaction and transport limitations.

The performance losses in an operating SOFC are:

- 1) Activation Losses(η_{act})
- 2) Ohmic Losses(η_{ohmic})
- 3) Concentration Losses(η_{conc})

Thus the operating voltage for a fuel cell can be expressed as,

$$V_{cell} = E - \eta_{act} - \eta_{ohmic} - \eta_{conc}$$

SOFC Efficiency

Fuel cell efficiency is defined as the ratio of useful energy generated to the total energy used by the process. The thermodynamic efficiency or ideal efficiency is given by,

$$\eta_{thermo} = \frac{\Delta G}{\Delta H} \quad (2.12)$$

Thermodynamic efficiency of the hydrogen fuel cell decreases as temperature increases because the entropy of reaction is negative. Real fuel cell efficiency is always less than ideal thermodynamic efficiency because of kinetic losses $\eta_{voltage}$ as well as fuel utilization losses η_{fuel}

The real efficiency of a fuel cell can be calculated by,

$$\eta_{real} = \eta_{thermo} \times \eta_{voltage} \times \eta_{fuel} = \frac{\Delta G}{\Delta H} \times \frac{V}{E} \times \frac{(i/n_e F)}{v_{fuel}} \quad (2.13)$$

Where V is the actual cell voltage, and v_{fuel} is the molar flow-rate of fuel supplied to the cell

2.1.3 Redox reaction in anode

Anode electrode is Ni (nickel) and YSZ (yttrium stabilized zirconia) as functional layer. Ni is being used as the electronic conductor as well as catalyst for the half reaction during the reaction Ni is converting in the NiO and vice versa reaction is as follows,



Reduction and oxidation of nickel will result in large bulk volume changes. In theory, the bulk volume of a fully dense NiO sample should contract by 40.9% upon reduction and should expand by 69.2% upon oxidation. [14] It is generally believed that NiO reduction is first-order and the rate has a linear dependence with the partial pressure of hydrogen but porous Ni-YSZ anode will not suffer such a tremendous volume change due to the existence of the pores. [14]

2.2 Flow equations and Boundary conditions

2.2.1 Flow in gas channels and electrode

The fluid flow in the channel is modeled using the weakly compressible form of the Navier-Stokes equation

$$\rho(v \cdot \nabla v) = -\nabla p + \nabla \cdot [\mu(\nabla v + (\nabla v)^T) - \frac{2}{3}\mu(\nabla \cdot v)I] \quad (2.15)$$

$$\nabla \cdot (\rho v) = 0 \quad (2.16)$$

Where v is velocity vector, μ is viscosity of fluid, ρ is the density, p is the pressure and I is the identity matrix.

Boundary Conditions

1. Mass flow rate is specified at inlet of air and fuel side
2. Gauge pressure is zero at both fuel and air exit
3. No slip boundary condition at the walls

$$v = 0|_{\partial\Omega_{walls}} \quad (2.17)$$

2.3 Mass Transfer in the channels and electrodes

The mass transfer equation or the convection-diffusion equation tracks the concentration for all gas phase species in the fuel /air channel and electrode.

$$\nabla \cdot j_i + \rho(v \cdot \nabla)w_i = r_i \quad (2.18)$$

Where w_i is the mass fraction and r_i is the mass source / sink term. r_i is non-zero only if current generation is allowed throughout the electrode. The diffusive flux j_i is given by the Maxwell Stefan Diffusion model.

$$j_i = -\sigma w_i \sum_{k=1}^n D_{ik}(\nabla y_k + (y_k - w_k)\frac{\nabla p}{p}) \quad (2.19)$$

Where n is the total number of species in the mixture, D_{ik} is the multicomponent diffusivity

Boundary Conditions

1. Mass fraction of H_2 in fuel and O_2 in air is specified at the fuel channel inlet and air channel inlet respectively.

$$wH_2|\partial\Omega_{fuel,inlet} = wH_{2,in}$$

$$wO_2|\partial\Omega_{air,inlet} = wO_{2,in}$$

2. No flux set at the wall of the channels

$$n \cdot J_i|\partial\Omega_{wall} = 0$$

2.4 Voltage and Current Distribution

The electronic and ionic potential in the electrode and electrolyte are modeled using the vector form of Ohm's law given by Poisson's equation.

$$\nabla \cdot (-\sigma_i \nabla \phi_i) = 0 \tag{2.20}$$

$$\nabla \cdot (-\sigma_i^{eff} \nabla \phi_i) = i_v \tag{2.21}$$

$$\nabla \cdot (-\sigma_e^{eff} \nabla \phi_e) = -i_v \tag{2.22}$$

where ϕ_i is ionic potential, ϕ_e is the electronic potential, σ_i is the ionic conductivity of the electrolyte, σ_i^{eff} is the effective ionic conductivity, and σ_e^{eff} is the effective electronic conductivity of the electrodes. i_v is the volumetric current generation in the electrodes. Equation (2.20) gives the ionic potential in the electrolyte and (2.21) and (2.22) gives the ionic and electronic potential in the composite electrodes.

Boundary conditions

1. Electric insulation or no flux at the electrode and electrolyte edges

$$n \cdot (\nabla \phi) = 0$$

2. Electric ground specified at the current collector of the anode i.e. $\phi_e = 0$
3. Electric ground specified at the current collector of the cathode i.e. $\phi_e = V_{cell}$

2.4.1 Effective Conductivity

Effective conductivity of electrode is calculated by coordination number and percolation theory. A detailed calculation of effective conductivity is given below: [2, 3, 13]

$$\sigma_{\alpha}^{eff} = \sigma_{\alpha}^0 [(1 - \phi_g)\psi_g P_g]^{\gamma} \quad (2.23)$$

Where σ_{α}^0 is conductivity of phase α in composite electrodes. ϕ_g is porosity of anode and cathode, ψ_g and P_g is volume fraction and percolation threshold of phase α , $\gamma = 3.5$ is the Bruggman factor. The conductivities (S/cm) of Ni and LSM are given by,

$$\sigma_{Ni}^0 = \frac{8.855 \times 10^5}{T} \exp\left(-\frac{9000}{RT}\right) \quad (2.24)$$

$$\sigma_{LSM}^0 = 3.27 \times 10^4 - 10.653T \quad (2.25)$$

The percolation threshold for phase α can be determined using equation,

$$P_{\alpha} = \left[1 - \left(\frac{4.236 - Z_{\alpha\alpha}}{2.473}\right)^{2.5}\right]^{0.4} \quad (2.26)$$

$Z_{\alpha\alpha}$ is the number of ionic and electronic particle neighbours and calculated as,

$$Z_{\alpha\beta} = \zeta_{\beta} \frac{Z_{\alpha} Z_{\beta}}{Z_{tot}} \quad (2.27)$$

Where Z_{tot} is average coordination number ($Z_{tot} = 6$ in a random packing of binary sphere).

The coordination numbers for the ionic and electronic conducting composite electrode can be calculated by

$$Z_{ed} = 3 + \frac{(Z_{tot} - 3)r_{ed}^2}{\zeta_{ed}r_{ed}^2 + \zeta_{el}r_{el}^2} \quad (2.28)$$

$$Z_{el} = 3 + \frac{(Z_{tot} - 3)r_{el}^2}{\zeta_{ed}r_{ed}^2 + \zeta_{el}r_{el}^2} \quad (2.29)$$

The number fraction of the electrode and electrolyte particle ζ_{ed} and ζ_{el} calculated as,

$$\zeta_{ed} = \frac{\psi_{ed}r_{ed}^3}{\psi_{ed}r_{ed}^3 + \psi_{el}r_{el}^3} \quad (2.30)$$

$$\zeta_{el} = \frac{\psi_{el}r_{el}^3}{\psi_{ed}r_{ed}^3 + \psi_{el}r_{el}^3} \quad (2.31)$$

The volume fraction of the electrolyte and electrode particle with respect to the solid phase can be calculated as:

$$\psi_{ed} = \frac{\phi_{ed}}{\phi_{ed} + \phi_{el}} \quad (2.32)$$

$$\psi_{el} = \frac{\phi_{el}}{\phi_{ed} + \phi_{el}} \quad (2.33)$$

2.4.2 Peclet number and Back diffusion

Peclet Number (Pe) is the ratio of convective flux to diffusive flux.

$$Pe = \frac{\text{Convective flux}}{\text{Diffusive Flux}}$$

By calculating Peclet Number which is a dimensionless number we can find convective flux is dominant. At less velocity diffusive flux is dominant along the length of fuel channel and fuel is diffusing before entering into reaction zone and waste of fuel. We need to maintain a minimum velocity at which convective flux is dominant along the fuel channel.

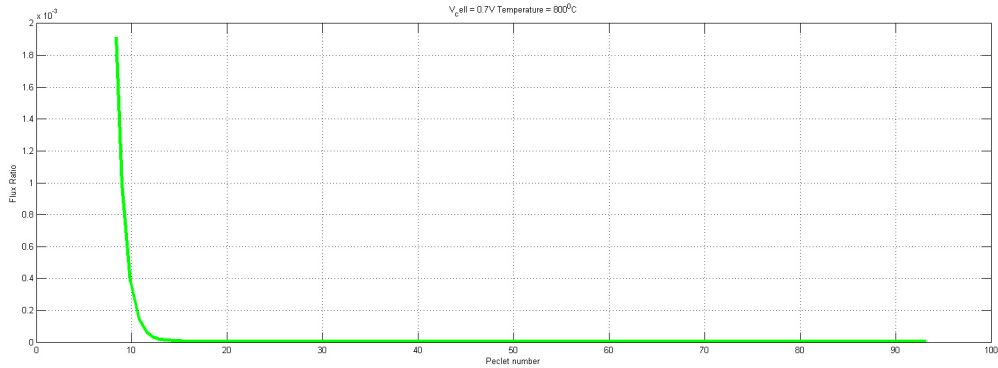


Figure 2.1: Flux ratio versus Peclet number

Flux ratio is ratio of diffusive flux of H_2 to total flux,

$$Fluxratio = \frac{DiffusivefluxH_2}{Totalflux}$$

Figure 2.1 shows a plot of flux ratio versus peclet number at temperature 700^0C and $0.7 V$ cell voltage, so we have kept peclet number more than a certain number where convective flux is dominant to diffusive flux. When the inlet flow rate is very low the back diffusion occurs and therefore the composition at interface of electrode and fuel is different from inlet composition. The back diffusion is more pronounced at low approach velocities. [13]

2.4.3 Electrochemistry

Thermodynamic dictates a maximum/reversible cell voltage, the voltage of an operating fuel cell is always less than Nernst voltage, because electrochemical reaction at each electrode requires a finite potential difference to generate current. The current generation is directly proportional to the rate of electrochemical reaction.

$$r_i = \frac{I}{n_i F} \quad (2.34)$$

Where r_i is the molar rate of reaction for species i and n_i is the number of electrons released/consumed per molecule of i, I is the current, and $F = 96485 C/mole$ is Faraday's constant.

The current generated is usually calculated using phenomenological equations such as the Butler Volmer equation for the hydrogen electro-oxidation reaction

$$i = i_0 \left\{ \frac{C_{H_2}}{C_{H_2in}} e^{\frac{-\alpha F}{RT} \eta_{in}} - \frac{C_{H_2O}}{C_{H_2Oin}} e^{\frac{-(1-\alpha)F}{RT} \eta_{in}} \right\} \quad (2.35)$$

Where i is the current density defined as $i = \frac{I}{A}$ where A is the apparent area of the electrode where the current is generated, i_0 is called the exchange current density and is a function of T and the inlet fuel composition. C_{H_2} is the concentration of H_2 and C_{H_2O} is the concentration of H_2O , α is the symmetry or charge transfer coefficient and $\eta_{in} = E - E_{in}$ is the anode activation over potential. E is the operating anode potential and E_{in} is the equilibrium anode potential at fuel inlet conditions.

$$E_{in} = E^0 + \frac{RT}{2F} \ln \frac{C_{H_2,in}}{C_{H_2O,in}} \text{ Anode}$$

$$E_{in} = E^0 + \frac{RT}{2F} \ln \frac{(C_{O_2,in})^{0.5}}{C_{O_2-}} \text{ Cathode}$$

2.5 Ni oxidation thermodynamics

Fuel cell produces water as product by consuming the hydrogen. Because of this water vapour production, we have reduction and oxidation of the nickel catalyst and electron conductor. Degradation of nickel is a cause of degradation in cell performance. To minimize the degradation of nickel we need to operate in favourable conditions. Nickel redox reaction depends on the partial pressure of the hydrogen and water vapour in the channel and porous electrode. To monitor the ration of partial of the in the channel we have a variable called P_{rat} .

$$P_{rat} = \frac{\text{mole fraction of hydrogen}}{\text{mole fraction of water vapour}}$$

It is important to calculate this ratio P_{rat} to study the Ni oxidation on anode surface. It can be calculated with the help of the thermodynamic feasibility of the gas.



We need to calculate the G of the reaction which gives the feasibility of the reaction. Where the NiO and Ni are the solids which are reacting with the gases. To calculate the ΔG of the reaction we have chosen the indirect way. We use the oxidation of the nickel with oxygen and formation of the water reaction to get the ΔG of reaction.



Adding equation 2.37 and 2.38 we get



To calculate the ΔG of the reaction 2.37 as function of temperature, we use the following relation [4] which is valid in our temperature range of operation.

$$\Delta G = -55844 + 20.290T \quad (2.40)$$

For water, Using a MATLAB routine of NASA polynomials we calculated the thermodynamic properties and ΔG value is calculated. The difference of both relation is the ΔG value for the nickel oxidation reaction in humid environment. According to the vants hoff relation,

$$\Delta G = \Delta G^0 + RT \ln(Q)$$

$$Q = \frac{ACTIVITYOFREACTANT}{ACTIVITYOFPRODUCT} = \frac{\partial PRESUREOFH_2O}{\partial PRESUREOFH_2}$$

$$\Delta G^0 = -RT \ln K$$

Final relation we can get as,

$$\Delta G = RT \ln \left(\frac{Q}{K} \right)$$

Knowing the value of ΔG^0 and the activities of reactants and products at any given condition, the free energy change for the equation at that condition, ΔG can be calculated, and the thermodynamic feasibility of the reaction can be predicted.

ΔG calculation for nickel oxidation using equation 2.40 at 1073K

$$\Delta G_{NiO} = -55844 + 20.290 * 1073 = -3.4073e+04 \text{ cal/mol} = -1.4253e+05 \text{ J/mol}$$

ΔG calculation for formation of water at 1073°K

By using a MATLAB routine of NASA polynomials we calculated ΔG for H_2 , H_2O and O_2

$$G_{H_2} = -1.5774e+05$$

$$G_{H_2O} = -4.6563e+05$$

$$G_{O_2} = -2.3874e+05$$

$$\Delta G_{H_2O} = G_{H_2O} - (G_{H_2} + G_{O_2})$$

$$\Delta G_{H_2O} = -4.6563e+05 - (-1.5774e+05 + (-2.3874e+05/2)) = -188520 \text{ J/mol}$$

For nickel oxide reduction

$$\Delta G^0 = \Delta G_{NiO} - \Delta G_{H_2O}$$

$$\Delta G^0 = -1.4253e+05 + 188520 = -45990$$

$$K = \exp\left(\frac{-\Delta G^0}{R \times T}\right)$$

$$K = \exp\left(\frac{45990}{8.314 \times 1073}\right) = 173.34$$

Therefore $K = 173.34$

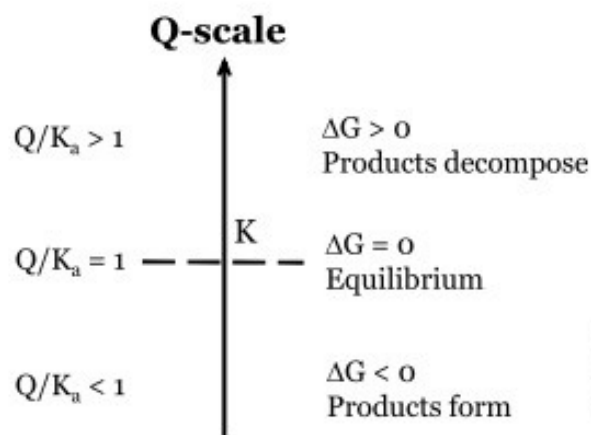


Figure 2.2: Scale for the ΔG and (Q/K) showing the spontaneous change of a chemical reaction

Chapter 3

Model Implementation

3.1 Geometry and Mesh

We are solving 2D planar cell and the geometry of cell is shown in the below figure.



Figure 3.1: 2D planar cell

This is the geometry we are built in COMSOL Multiphysics 4.3b and dimensions are mentioned in parameter.

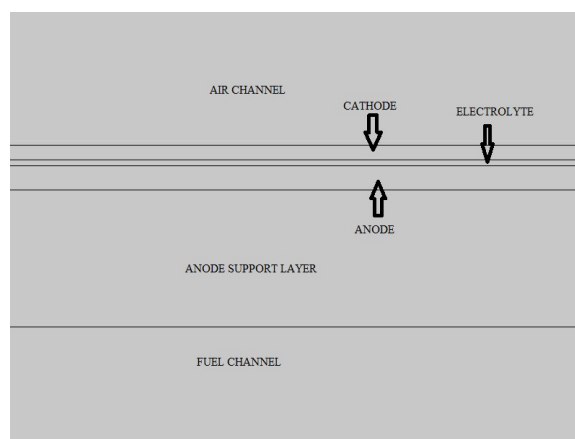


Figure 3.2: fuel cell 2-D section of actual simulated geometry

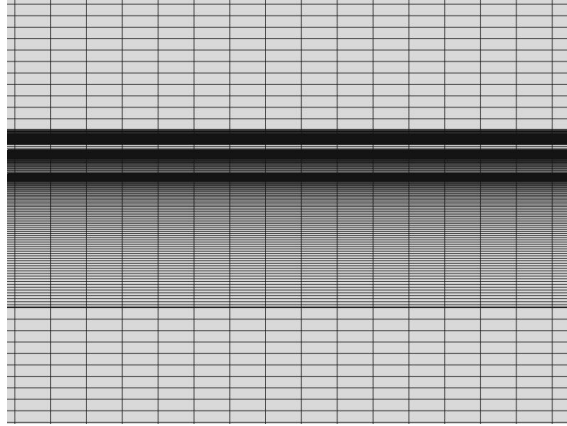


Figure 3.3: 2D planar cell meshing

We use a mapped mesh and mesh density is controlled by specifying the number of grid points at boundaries of electrode, electrolyte and channel. Mesh distribution is shown in figure 3.3. We used a 2D mesh with 90850 elements. The simulation convergence is mostly depends upon mesh sizes on perpendicular boundary of electrode-electrolyte.

3.3 Solver Used

COMSOL Multiphysics 4.3b software are used for simulation. We are simulating the 2D geometry fuel cell with fully coupled model with study parameter like cell voltage, fuel flow rate, temperature. [15]

3.2 Parameter

Table 3.1: These are the parameters

Parameter	Value	Units
Anode		
Thickness	550	μm
Exchange current density	8.5	A/cm^2
YSZ particle radius	0.5	μm
Ni particle radius	0.5	μm
Porosity	0.35	
Anode symmetric factor (α_a)	1.5	
Cathode symmetric factor (α_c)	0.5	
Permiability of anode	1.97×10^{-11}	m^2
Cathode		
Thickness	50	μm
Exchange current factor	2.8	A/cm^2
YSZ particle radius	0.25	μm
LSM particle radius	0.75	μm
Porosity	0.35	
Anode symmetric factor (α_a)	0.75	
Cathode symmetric factor (α_c)	0.5	
Permeability of cathode	1.975×10^{-11}	m^2
Electrolyte		
Thickness	10	μm
Gas flow channel height	1×10^{-3}	m

Chapter 4

Results and Discussion

A 2D planar cell and a parametric study at different temperatures, cell voltage, fuel flow rate has been studied and discussed in detail. A safe region has been observed where nickel oxidation is not taking place and is shown in graphs.

Results for two different inlet fuel composition at different temperatures are discussed in section below.

4.1 $H_2 : H_2O = 0.97:0.03$

Simulations have been run for 2D planar model at 700°C, 750°C, 800°C.

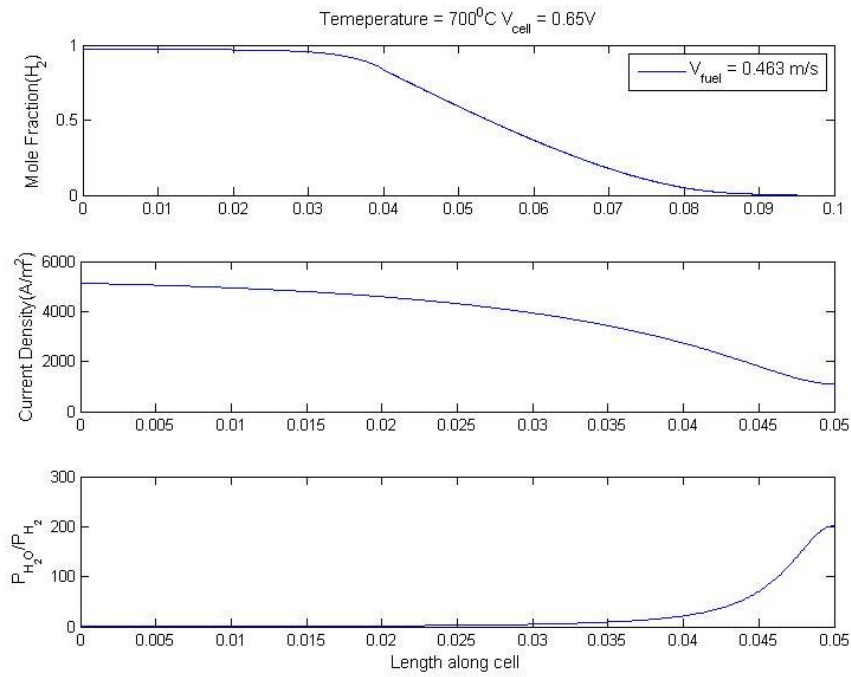


Figure 4.1: Mole Fraction of H_2 , current generation and partial pressure along the length of cell at 700°C

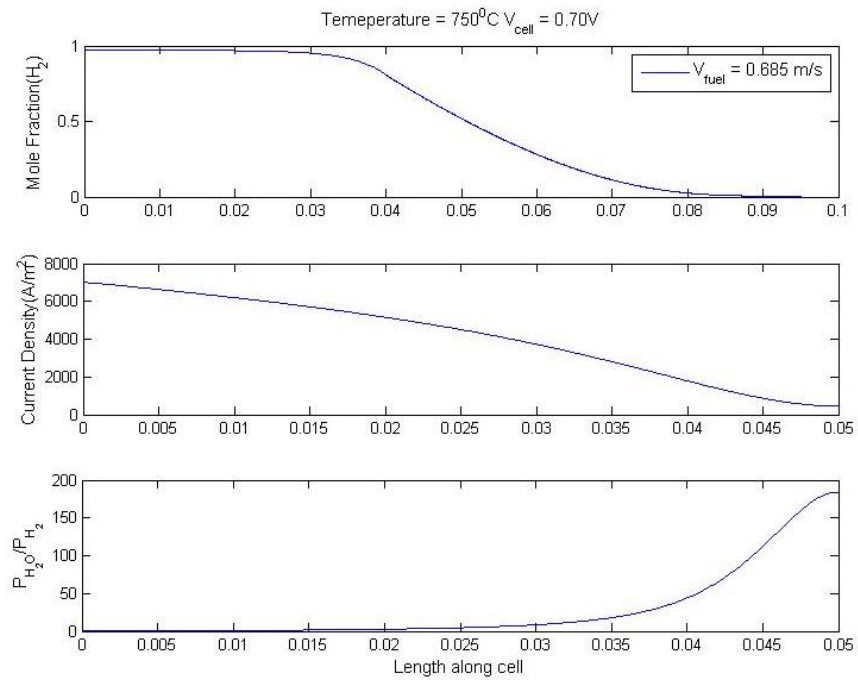


Figure 4.2: Mole Fraction of H_2 , current generation and partial pressure along the length of cell at 750°C

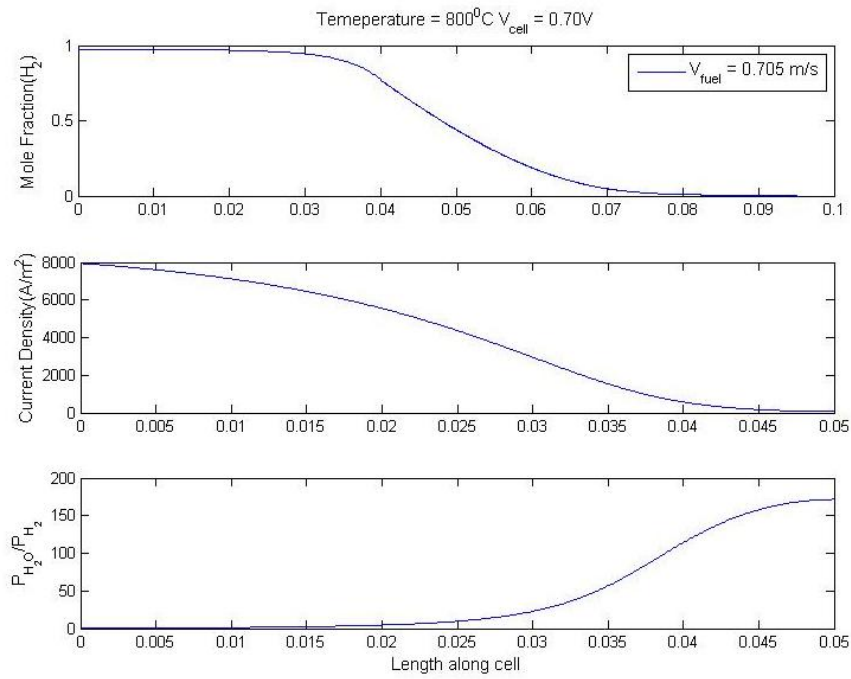


Figure 4.3: Mole Fraction of H_2 , current generation and partial pressure along the length of cell at $800^\circ C$

Figures 4.1, 4.2 and 4.3 shows the mole fraction of H_2 , current density and partial pressure ratio with respect to length along the cell at $700^\circ C$, $750^\circ C$ and $800^\circ C$. They are plotted at a velocity where fuel utilization is more than 99% but no nickel formation. Beyond this limit of fuel utilization nickel oxidation will take place.

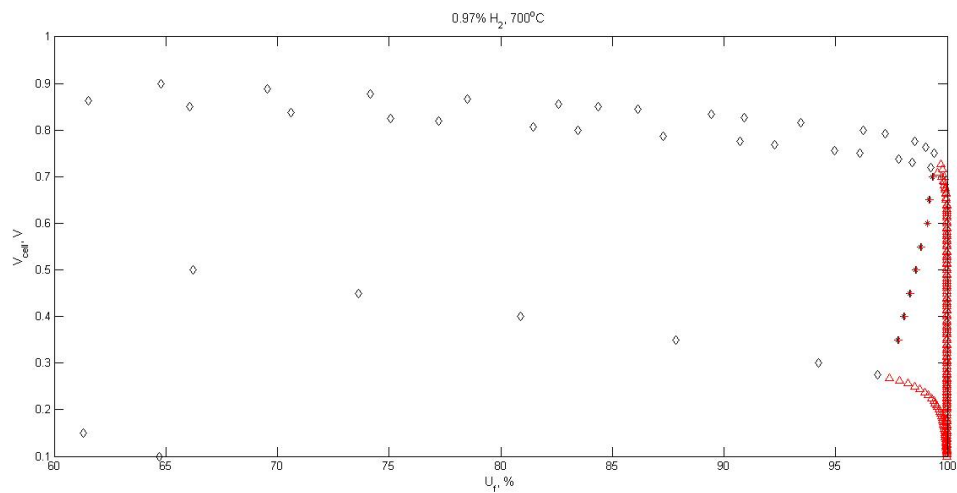


Figure 4.4: Safe and Unsafe region for $700^\circ C$

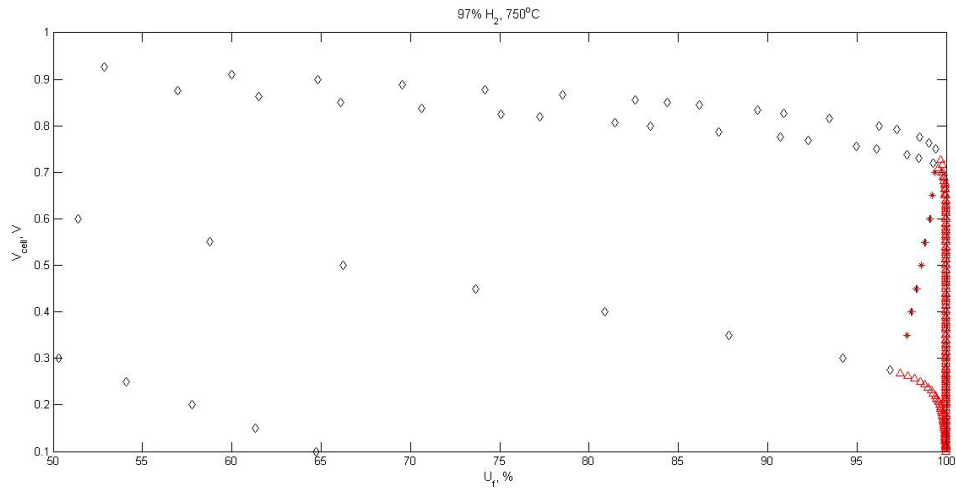


Figure 4.5: Safe and Unsafe region for 750⁰C

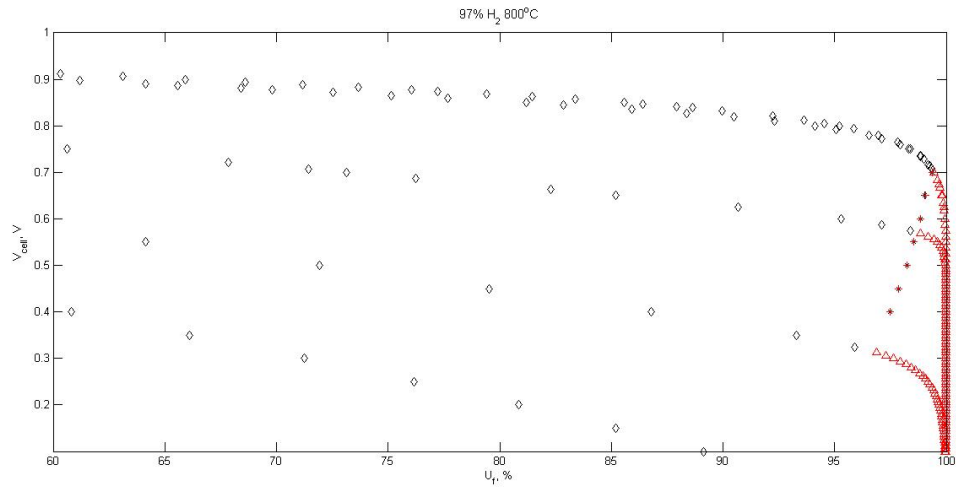


Figure 4.6: Safe and Unsafe region for 800⁰C

Figures 4.4, 4.5 and 4.6 are the plots of cell voltage vs utilization curve at 700⁰C 750⁰C and 800⁰C which predicts the safe operating condition to avoid nickel oxide formation. Red points denote unsafe operating condition where nickel oxidation takes place and black points denote safe operating condition. For safe and unsafe operating condition, fuel flow rate also plays an important role. As fuel flow rate is increasing, utilization is decreasing and at less fuel flow rate, formation of nickel oxidation is taking place. In all the three cases the ratio of $H_2 : H_2O$ is 0.97:0.03.

2. $H_2 : H_2O$ 0.55:0.45

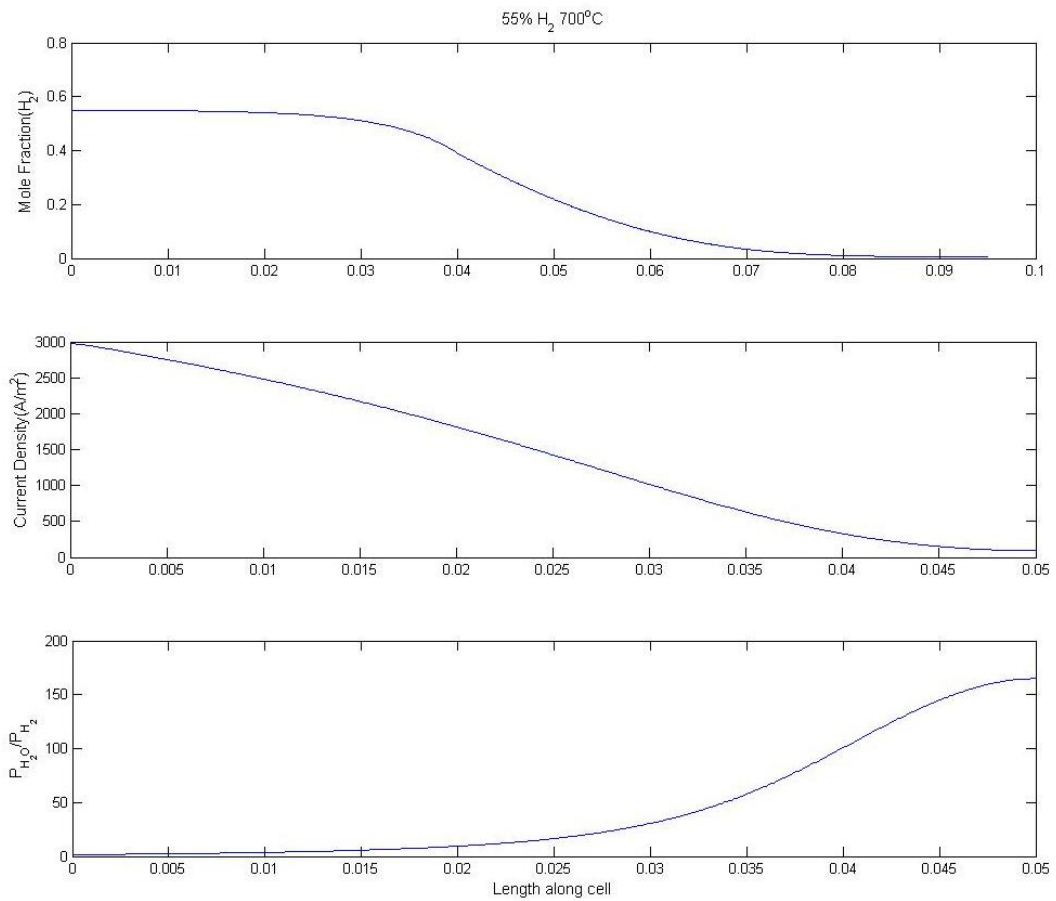


Figure 4.7: Mole Fraction of H_2 , current generation and partial pressure along the length of cell at $700^\circ C$

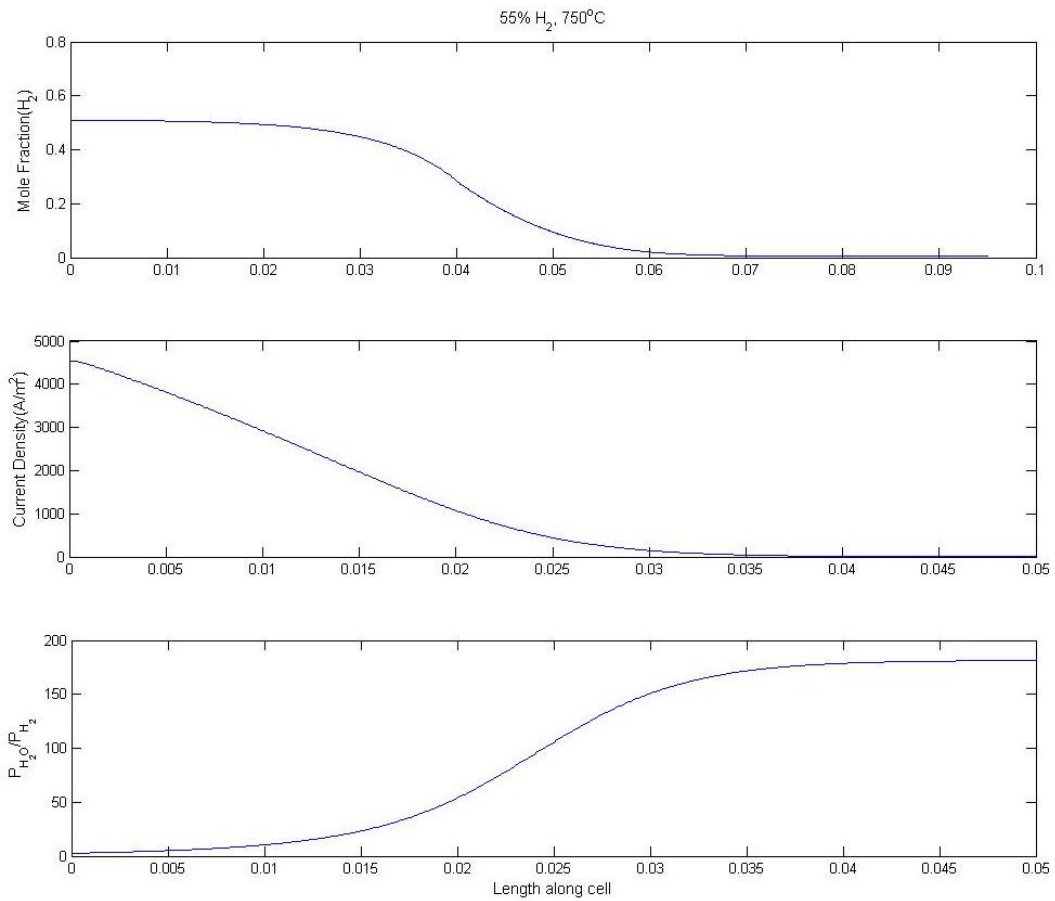


Figure 4.8: Mole Fraction of H_2 , current generation and partial pressure along the length of cell at $750^\circ C$

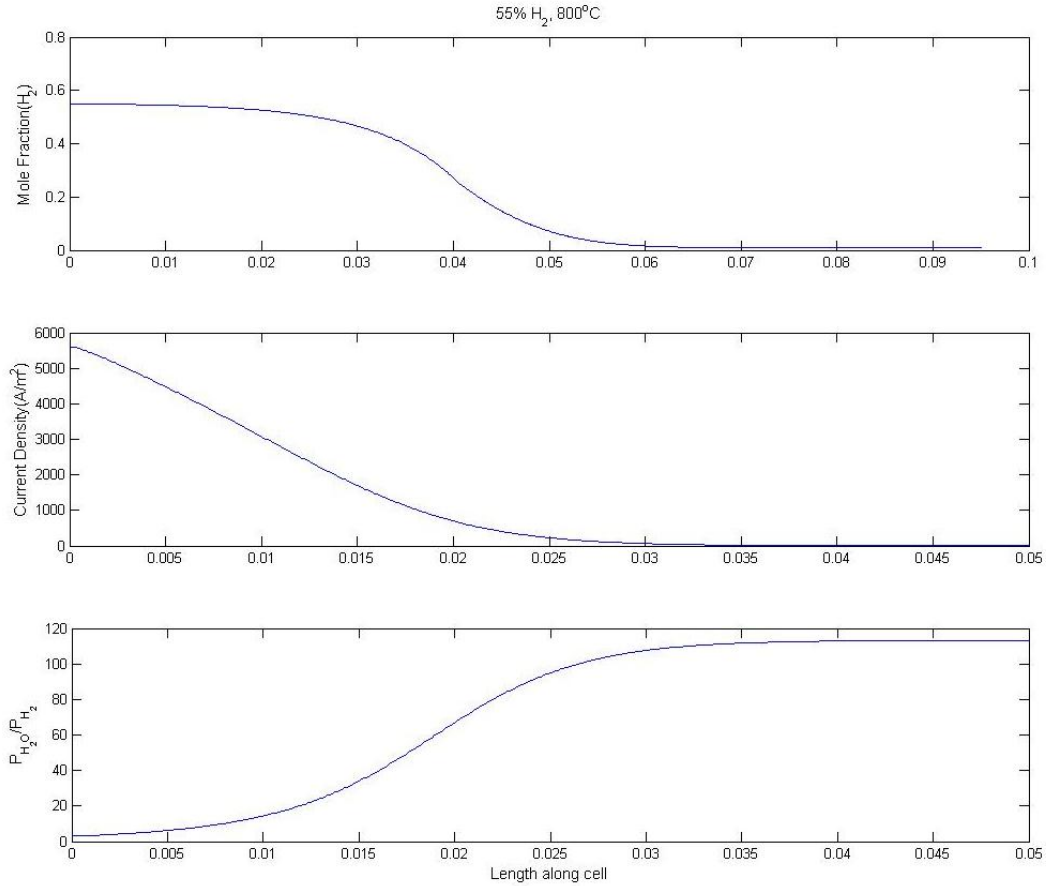


Figure 4.9: Mole Fraction of H_2 , current generation and partial pressure along the length of cell at $800^{\circ}C$

Figures 4.7, 4.8 and 4.9 show the mole fraction of H_2 , current density and partial pressure ratio with respect to length along the cell at $700^{\circ}C$, $750^{\circ}C$ and $800^{\circ}C$. They are plotted at a velocity where utilization is more than 98% with no nickel formation. But compared to figures 4.1, 4.2 and 4.3 current generation is on half of the length of the cell, because the inlet composition $H_2 : H_2O$ is 0.55:0.45. So when fuel is electrochemically oxidized along the length of anode channel, fuel consumed in the anode fuel stream is diluted by the reaction product (like H_2O). Figures 4.8 and 4.9 shows that only half of the cell is active.

As the fuel concentration decreases along the length of the anode channel, reversible potential decreases.

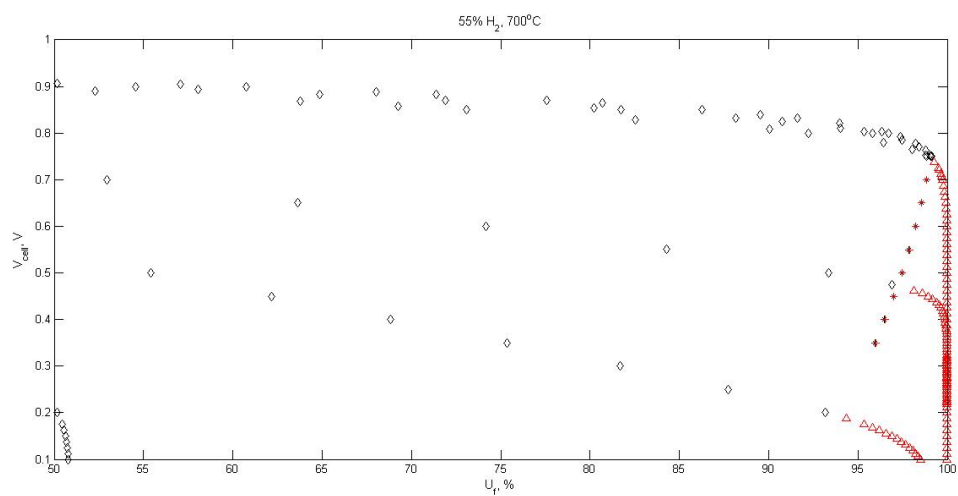


Figure 4.10: Safe and Unsafe region for 700°C

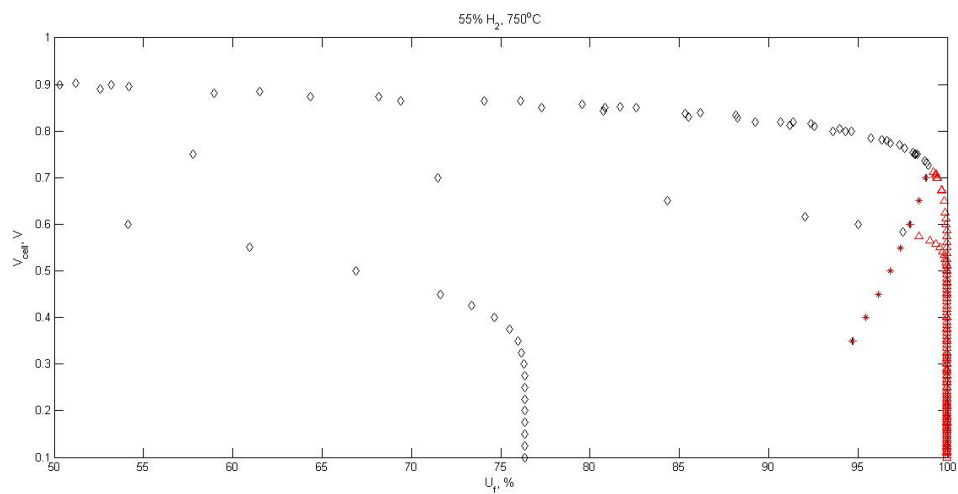


Figure 4.11: safe and Unsafe region for 750°C

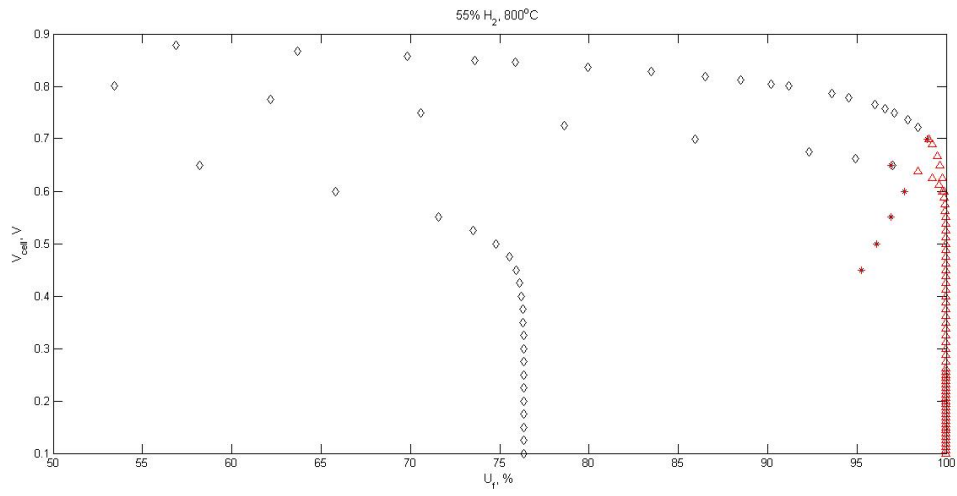


Figure 4.12: Safe and Unsafe region for 800°C

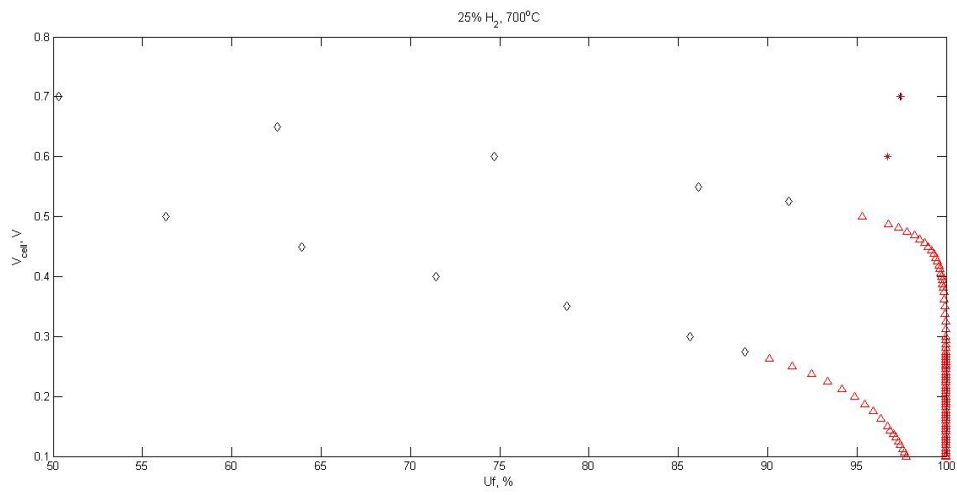


Figure 4.13: Safe and Unsafe region for 700°C at H_2 25%

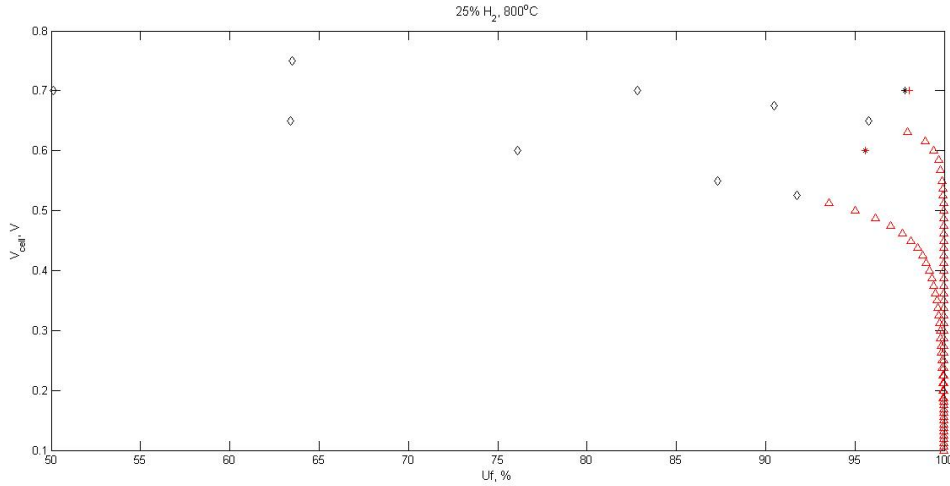


Figure 4.14: Safe and Unsafe region for 800°C at H_2 25%

Figure 4.10, 4.11 and 4.12 shows cell voltage vs utilization curve 700°C 750°C and 800°C which predicts the safe operating condition where nickel oxide formation is not taking place. Red points in the plots denote unsafe operating condition where nickel oxidation takes place and black points denote safe operating condition. For safe and unsafe operating condition fuel flow rate also plays an important role. As fuel flow rate is increasing, fuel utilization decreases and at less fuel flow rate nickel is oxidised. In all three cases, the ratio of $H_2 : H_2O$ is 0.55:0.45

Figures 4.1, 4.2 and 4.3 conclude that according to the inlet composition of fuel stream, at $H_2 : H_2O = 0.97:0.03$, nickel oxidation is happening after 99% of fuel utilization. At a very less velocity with ratio Q/K greater than 1 and it is observed that whole length of the cell is active which can be seen in figures 4.1, 4.2 and 4.3 for second plot which are current generation plots

But for composition $H_2 : H_2O = 0.55:0.45$, nickel oxidation occurs after 98% fuel utilization. At low velocity with ratio Q/K greater than 1 and where whole length of the cell is not active, current is generated along the half length of the cell. As fuel reacts along the length of cell anode fuel stream gets diluted by H_2O which can be seen clearly in Figures 4.7, 4.8 and 4.9.

Figures 4.13 and 4.14 shows safe and unsafe region for a composition of $H_2 : H_2O = 0.25:0.75$. At 700°C Nickel oxidation takes place after 90% fuel utilize when compared to 95% at 800°C. So at 800°C we can utilize maximum fuel with safe operation without nickel oxidation.

Nickel Oxidation also depends on partial pressure of hydrogen and water vapour in the channel and porous electrode. A variable $Prat$ is defined as the ratio of mole fraction of hydrogen to mole fraction of water vapour which is given in section 2.10

$$Prat = \frac{\text{mole fraction of hydrogen}}{\text{mole fraction of water vapour}}$$

This ratio depends on operating temperature of the cell. In the above Figures 4.1, 4.2, 4.3, 4.7, 4.8 and 4.9, all third plots denote $\frac{P_{H_2O}}{P_{H_2}}$ along the length of the cell. If this ratio is high, nickel is oxidised. So to prevent nickel oxidation ratio should be below threshold as dictated by thermodynamics of Ni oxidation as mentioned in section 2.5.

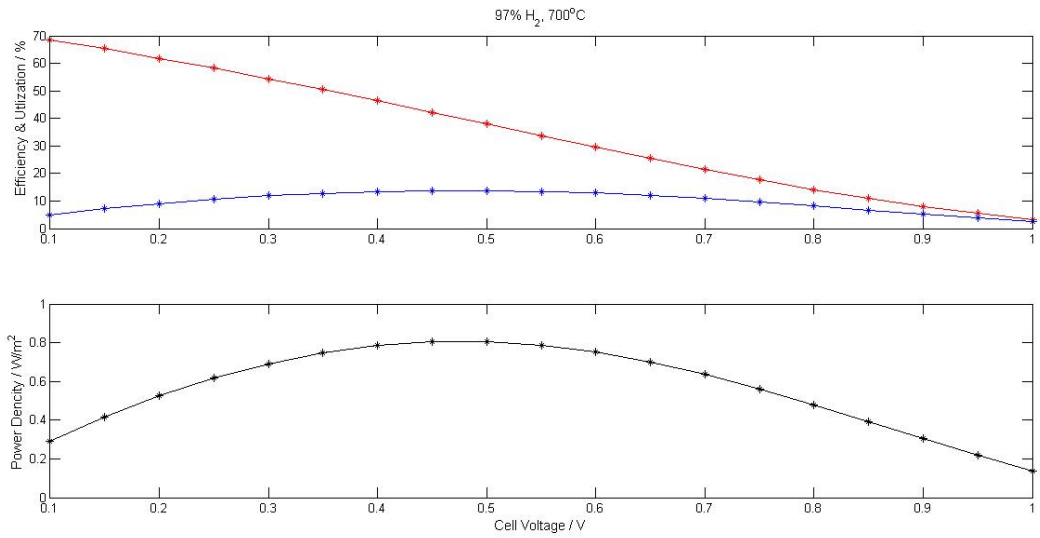


Figure 4.15: Fuel cell efficiency as function of cell voltage at a given utilization at 700°C

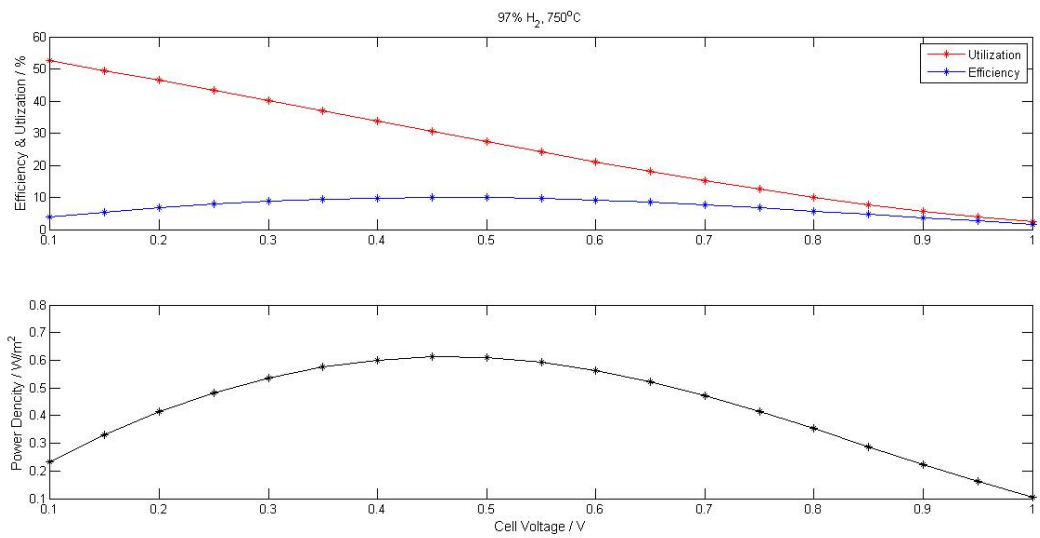


Figure 4.16: Fuel cell efficiency as function of cell voltage at a given utilization at 750°C

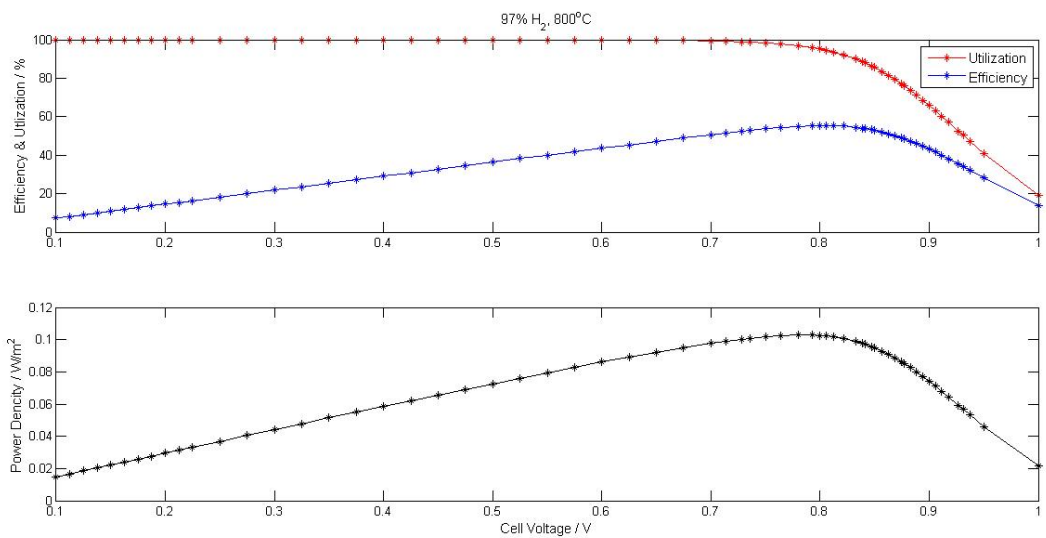


Figure 4.17: Fuel cell efficiency as function of cell voltage at a given utilization at 800°C

Figures 4.15, 4.16 and 4.17 shows a fuel cell efficiency and power density is function of cell voltage at a given utilization for three different temperature. When cell is operated at low voltage which can produce high current but there are two things which play an important role, which are cell efficiency and fuel utilization. A particular voltage will give maximum cell efficiency and fuel utilization. From the figures 4.15, 4.16, 4.17, If cell is operated at 0.7V to 0.8V voltage range we will have maximum cell efficiency and maximum fuel utilization.

Chapter 5

Conclusion

In this thesis we presented a 2D planar model of Solid Oxide Fuel Cell. The model include all physics, thermodynamics, mass transfer, transport phenomena. This model is a fully coupled detailed reaction transport model of solid oxide fuel cell model.

To find out safe zones for cell operation, the cell has been simulated for different temperature, fuel flow rate and composition and voltages ranges.

1. From the safe and unsafe zone we can predict the desirable operating conditions for different temperatures and voltages.
2. Fuel inlet flowrate has a direct effect on fuel utilization. At higher fuel flow rates fuel utilization is low and at lower fuel flow rates fuel utilization is high and at higher fuel utilization Ni oxidation might take place. So, at lower fuel flow rates Ni oxidation might take place.
3. Nickel oxidation depends upon the ratio of partial pressure of hydrogen and water vapour. Towards the end of the cell length Q/K is less than 1 which indicates Ni oxidation taking place and that leads to deterioration of anode. From safe and unsafe region plots we can decide the safe operating condition where nickel oxidation is not taking place during the cell operation.
4. For all the simulation in this study, the threshold U_f increases with increasing cell voltage V_{cell} .
5. With increasing dilute fuel, the threshold U_f increasing from 98% for fuel with 97% H_2 to 96% for 25% H_2

References

- [1] O'Hyare Ryan, Cha Suk-Won, Colella Whitney, Prinz Fritz B, *Fuel Cell Fundamental, John Wiley and Sons* 2nd ed, (2009)
- [2] Zhu Huayang, Kee Robert, Modeling Distributed Charge-Transfer Processes in SOFC Membrane Electrode Assemblies *Journal of Electrochemical Society*, 155 (2008) B715-B729
- [3] Zhu Huayang, Kee Robert J, Janardhanan Vinod M, Deutschmann Olaf and Goodwin David G, Modeling Elementary Heterogeneous Chemistry and Electrochemistry in Solid-Oxide Fuel Cells. *Journal of Electrochemical Society*, 152 (2005) A2427-A2440
- [4] Carette G.G, Flengas S. N, Thermodynamic Properties of the Oxides of Fe, Ni, Pb, Cu and Mn by EMF Measurements *Department of Metallurgy and Material Science, University of Toronto, Canada.*
- [5] Zhu Huayang, Kee Robert J, Thermodynamics of SOFC efficiency and fuel utilization as function of fuel mixtures and operating conditions. *Journal of Power Sources* 161 (2006) 957-964
- [6] Monder D S, Modelling Studies for Hydrogen Sulphide Fuelled SOFC's, PhD thesis *University of Alberta, Edmonton Canada, 2008*
- [7] Shekhar Rustam S. (2014), Fuel utilization and its effect on solid oxide fuel cell performance, M.Tech thesis, IIT Hyderabad, India.
- [8] Kumar S. (2013), A fully coupled transport-reaction model for a solid oxide fuel cell, M.Tech thesis, IIT Hyderabad, India.
- [9] Neidhardt J P, Nickel Oxidation in Solid Oxide Cells: Modeling and Simulation of Multi-Phase Electrochemistry and Multi-Scale Transport, Thesis 2013
- [10] Neidhardt J, Henke M, Bessler W G, Kinetic Modeling of Nickel Oxidation in SOFC Anodes *Electrochemical Society* 35(1) (2011) 1621-1629

- [11] Neidhardt J P, Yurkiv V, Bessler W. G, Spatiotemporal simulation of nickel oxide and carbon phases formation in solid oxide fuel cell
- [12] Jonathan Neidhardt, Moritz Henke and Wolfgang G. Bessler, Kinetic Modeling of Nickel Oxidation in SOFC Anodes. *ECS Transaction* 35(1) (2011) 1621-1629
- [13] Janardhanan V M, Deutschmann O, Modeling diffusion limitation in solid oxide fuel cells. *Electrochimica Acta* 56 (2011) 9775-9782
- [14] Yun Zhang, Bin Liu, Baofeng Tu, Yonglai Dong, Mojie Cheng, Understanding of redox behavior of Ni - YSZ cermets *Solid State Ionics* 180 (2009) 1580-1586
- [15] COMSOL. COMSOL Multiphysics help documentation, COMSOL 4.3b, 2013.